Chapter 5

Gamma Uranium Molybdenum Alloy: Its Hydride and Performance

Enrique E. Pasqualini

Additional information is available at the end of the chapter

http://dx.doi.org/10.5772/63652

Abstract

The high density metastable gamma uranium molybdenum alloy (γ-UMo) is being qualified as a nuclear fuel for the conversion of high enriched uranium (HEU) to low enriched uranium (LEU) fuels in research nuclear reactors. γ-UMo, with compositions between 7 and 10 wt.% molybdenum, has excellent properties to allocate fission gases but unacceptable behavior in contact with aluminum in the matrix of dispersed fuels. Development and processing alternatives are welcome to decide final working paths and new nuclear fuels design. A historical introduction on the development of materials testing reactors (MTR) nuclear fuels is presented to illustrate comings and goings to reach desired qualification objectives. Several studies performed on UMo probes, miniplates and full size plates are mentioned to contribute to the knowledge of fuel properties and to incorporate new process technologies. Focus is directed to the discovery of the gamma uranium molybdenum hydride and the hot rolling colamination of monolithic UMo with nonaluminum claddings. A scalable process of hydriding, milling and dehydriding (HMD) to comminute the ductile UMo was developed. Monolithic UMo miniplates with Zircaloy-4 (Zry4) cladding was colaminated for the first time and under irradiation conditions showed excellent performance after high burn-up.

Keywords: uranium, molybdenum, zircaloy-4, hydride, comminution, colamination, coverage

1. Introduction

Nuclear reactors can be divided into two types: those used to produce electrical power and those for other purposes. Power reactors take advantage of the energy liberated in the fission of fissile nuclides (^{235}U, ^{239}Pu) to produce electricity and nonpower reactors are used for training and

mainly uses the neutrons produced in the fission reactions for materials testing, fuel qualification, radioisotope production, neutron activation analysis, neutron diffraction, silicon transmutation, research, etc. Actually, there are 442 operating nuclear power reactors in 33 countries around the world, while 66 are being constructed [1]; those used for naval propulsion are not recorded. Modern nuclear power reactors can generate more than 1000 MW of electrical power and one important characteristic of this type of reactors is that they work at temperatures higher than 300°C and usually at very high pressures [2]. Nonpower reactors are nominated by their maximum thermal power generated, which is proportional to neutron density; thermal power ranges go from practically zero up to some tens of MW, reaching in some cases powers of several hundreds of MW and fluxes greater than 10^{14} neutrons.cm^{-2}.s^{-1}. In these nonpower reactors, working temperatures are normally near room temperature; for very high density powers, maximum temperatures at the center of these high surface to volume ratios, fuel units do not surpass 200°C. There are 248 operating nonpower reactors in 52 different countries around the world [3].

Considering the different requirements to which both kinds of reactors are subsumed, the corresponding nuclear fuels have different characteristics. Typical operating power densities in power reactors are usually higher than 100 kW/l; in the case of nonelectrical power reactors, operating power densities can reach values as high as 1000 kW/l. Power reactors have their fuel material in the form of oxides, basically UO_2, with ^{235}U enrichment lower than 5%, in pellet form filling a zirconium alloy tube. Nonpower reactors have usually plate-like fuels, or pins, with some uranium compound powder dispersed in an aluminum matrix and with an aluminum alloy cladding. Seventy-six research reactors use high enriched uranium fuels (HEU > 90% ^{235}U) [4] and the remaining ones use low enriched uranium (LEU < 20% ^{235}U) fuel.

Actually, there is an important interest that the reactors that are working with HEU fuels be converted to LEU, trying to not affect their performance. The reason is to diminish proliferation risks since HEU is used for the construction of nuclear weapons.

1.1. The beginnings of testing reactors, 1948–1978

One of the first necessities in the development of power reactors was to acquire knowledge on the behavior of irradiated materials and devices. For these purposes, materials testing reactors were constructed. The greatest interest for this purpose, by the beginning of the 1950s, was to obtain thermal neutron fluxes higher than 10^{14} n.cm^{-2}.s^{-1}, high specific power and high excess reactivity, with the possibility of configuring slab geometries of the nuclear core so as to obtain particular neutron spectra [5, 6]. The reactor nucleus had a volume of 100 liters with a total power of 30 megawatts. The fuel elements with 200 grams of ^{235}U were assemblies of 19 hot colaminated curved plates brazed into slotted lateral plane plates [7]. The plates had inside a monolithic aluminum alloy with HEU shaping a dispersion of UAl_4 precipitates in a rich aluminum matrix and aluminum cladding. The monolithic meat had a total uranium density of 1.6 gU/cm^3. The typical size of the plates was 1.4 x 69 x 555 mm with a cladding thickness of 0.46 mm. Separation between plates was 2 to 3 mm with cooling water flowing between them at a velocity of 10 ms^{-1}.

http://dx.doi.org/10.5772/63652

Plates were also developed using powder metallurgy technology [8] with UO_2 dispersed in aluminum and in stainless steel obtaining higher charges of uranium densities. Maximum heat fluxes were 32 W/cm^2 in the case of aluminum plates working at 93°C and 70 W/cm^2 in the case of stainless steel plates working at 290°C. These power densities are equivalent to a maximum specific power of 2 kW/g of ^{235}U. Stainless steel plates had total and cladding thicknesses of 0.7 and 0.12 mm, respectively [9]. Plutonium and ^{233}U charged fuel plates were also developed [10].

At those early times, reactors with LEU were proposed showing that the critical mass does not increase significantly over that obtained using HEU; some metallurgical problems have to be reconsidered to fabricate in the highly concentrated combination required [11]. Tubular geometries of plate-like fuels were also used. Pool-type reactors and pressurized vessels were constructed. Channel-type reactors had different positions to obtain desired neutron fluxes and spectra avoiding fuel elements reconfigurations. Many other experiences were encouraged but the ones mentioned have many of the basic elements that are used up today in the fuel nuclear industry.

1.2. Enrichment reduction of nuclear fuels start up, 1978–1996

After India exploded a nuclear bomb in May 1974 a nonproliferation International Nuclear Fuel Cycle Evaluation (INFCE) was set up [12]. The Reduced Enrichment for Research and Test Reactors (RERTR) Program was released in 1978 to "develop technology necessary to enable the conversion of civilian facilities using HEU to LEU fuels and targets" [13]. The reason to adopt this criterion is that LEU is considered to be less of a proliferation concern than HEU because the critical mass—without neutron moderation—increases rapidly below 20% ^{235}U. One of the first fuels to be developed as nonproliferate was the French Caramel that consisted in plates with thin square slabs of UO_2—with uranium enrichment lower than 10% placed in a square pitch grid of zircaloy and welded between two zircaloy sheets [14]. The total uranium density of this fuel is 10.3 gU/cm^3 and takes advantage of the experience gained in power reactors. Because of low conductivity of the oxide, thin square type slabs were developed. Fuels with uranium oxides and silicides dispersed in aluminum had at that time less known performance. It is interesting to revisit some of the initial review works that followed the consolidated policy of enrichment reduction [15]. In this guidebook of 1980, preferred high density fuels were mentioned, such as U_3Si, UMo alloys and UO_2.

Experience can also be gathered from the design of nuclear fuels for naval propulsion, where several uranium compounds and enrichments were reviewed. As an example it can be mentioned that uranium with 10 wt.% (21.6 at.%) molybdenum alloys were used in fast reactors without surpassing 2% burn up because of excessive fission gas induced swelling that occurs at temperatures greater than 400°C [16]. It is also mentioned that in comparison with uranium niobium and uranium zirconium alloys, at lower temperatures, UMo alloys are apparently more resistant to swelling.

It was inevitable to move on to powder metallurgy to incorporate to the fuel more uranium to compensate the ^{235}U lower concentration. This technology was already known since dispersion fuel elements present several advantages over elements containing the fuel in homogeneous ceramic form [17]. Also it was in mind trying to use high density uranium compounds. In the

case of uranium alloy worked as a monolithic meat with UAl_4 precipitates, the uranium loading must be less than 35 wt.% uranium (4 at.% U)—to avoid inhomogeneous dispersions that could produce hot spots—rendering a final meat density of 1.35 gU/cm^3 of total uranium. In the case of a UAl_x (x = 2, 3 or 4) dispersed powder in an aluminum matrix with a concentration between 40 and 50 v/v%, densities of total uranium in the meat can reach values higher than 2 gU/cm^3.

One of the simplest choices to increase fuel density was to develop fuel plates with LEU U_3O_8 dispersed powder in an aluminum matrix. The density of U_3O_8 is 8.3 g/cm^3 and the meat total uranium density can reach values higher than 3.1 gU/cm^3. Dispersed UO_2 powder in an aluminum matrix is less stable than U_3O_8 since important swelling is formed due to low density reaction products and diffusion porosity formed [17].

Uranium silicide compounds such as U_3Si and U_3Si_2 have different behavior under irradiation. While the first one presented in some cases break away swelling [18], U_3Si_2 was finally selected to rich total uranium densities at the fuel plate meat of 4.8 gU/cm^3 [19]. This fuel is the last one that has been qualified for general uses in research reactors using LEU. It is worthwhile to comment that U_3Si is a ductile compound and centrifugal atomization [20] was specially dedicated to obtain a ductile compound in powder form.

1.3. Uranium molybdenum long run qualification

By 1996, in a systematic study, several high density uranium compounds were revisited to be used as nuclear fuels with the intention of reducing even more the utilization of HEU in research reactor fuels and to look for a fuel more easily reprocessed than the U_3Si_2 dispersions [21, 22]. Some of these compounds to be qualified resulted to be gamma stabilized uranium alloys [23], in particular the metastable phase γ-UxMo. Quickly, it was determined in irradiation experiments that the needed composition had to have more than 6% w/w Mo (x > 6) [24]; afterwards it was observed that γ-UMo had an exceptional behavior in the allocation of fission gas bubbles [25]. UxMo alloys, with weights percent between seven and ten ($7 \leq x \leq 10$), are being tested since the stability of the gamma phase is enhanced as molybdenum concentration increases [26, 27], favoring intermediate fabrication processes. UMo presents interface incompatibilities with aluminum at high irradiation fluxes when fission gases generate undesired porosity [28–30]; this drawback is diminished by the incorporation of silicon to the aluminum matrix [31]. Fuel/cladding interaction can be minimized by covering the fuel particles with a diffusion barrier material or tailoring the fuel or matrix materials with the incorporation of additional alloying elements.

Since γ-UMo is a ductile alloy, it can be used as a monolithic fuel; nevertheless it cannot be colaminated with aluminum because of the different thermomechanical properties of both materials [32]. Several alternatives have been proposed to obtain a γ-UMo monolithic fuel with aluminum cladding [33]. They comprise a first step in which UMo foils are hot laminated to final dimensions and a second step is the incorporation of the aluminum cladding that can be performed by transient liquid phase bonding, friction stir welding or hot isostatic pressing. All of these three alternatives have UMo/Al interfaces where fission gas bubbles can coalescence. To avoid a UMo/Al interface a zirconium diffusion barrier can be incorporated between

http://dx.doi.org/10.5772/63652

both materials and afterwards hot pressed to complete an aluminum cladding [34]. Irradiation results can be obtained in more detailed overviews [35].

2. γ-UMo massive hydride discovery and powder production

Several methods have been used to comminute UMo alloys: the more sophisticated centrifugal atomization already mentioned from KAERI, mechanical grinding performed initially in Canada and rotating electrode [36]. Studies of gaseous atomization with gold used as surrogate material to evaluate production performance were also performed [37]. Another explored possibility of comminuting UMo ductile alloys is by the decomposition of metastable γ-UMo in α-U and U_2Mo by a controlled heat treatment. When an incipient cellular precipitation totally decorates grain boundaries, the α-U phase present can be hydrided. The brittle hydride weakens the material that can easily be milled to particles of dimensions similar to the original grain size [38, 39].

Increasing the temperature of a quenched melted rod of U7Mo in a hydrogen atmosphere, hydrogen pick up started at around 100°C; the incorporation went higher than the hydrogen solubility limit and before decomposition of the metastable gamma phase took place [40,41]. It could be observed that a new phase begun to form at the place where tensile stresses were bigger. With this input, the method to completely hydride the γ-UMo alloy was developed. An hydriding, milling and dehydriding method, HMD, was set forward to obtain γ-UMo powder [42, 43].

2.1. Casting of UMo with stress retention

Batches of up to one kilogram of alloy were prepared with natural uranium (>99.7% U) and LEU (>99.9% U). Lumps of metallic uranium and molybdenum chips were used to prepare a 7% w/w molybdenum alloy. Uranium was deoxidized using nitric acid and molybdenum with melted sodium hydroxide. A high frequency induction furnace was used for melting the alloy in magnesium oxide crucibles and an inert gas atmosphere.

The melt was poured in a graphite dish obtaining a circular plate of approximately 8 mm thick and 120 mm diameter. Tension stresses at the top of the plate are retained since solidification begins at the bottom in contact with the graphite. The plate is finally broken in pieces (**Figure 1**) such that they can be incorporated in a hydriding chamber.

Residual tension stresses at the upper surface were checked by peak displacement in X-ray diffractions (DRX) in the as melted condition and after an annealing treatment (**Figure 2**). These stresses in the γ-UMo alloy are needed to allow the initiation of hydriding.

Figure 1. Eight millimeters thick uranium molybdenum lumps with residual stresses.

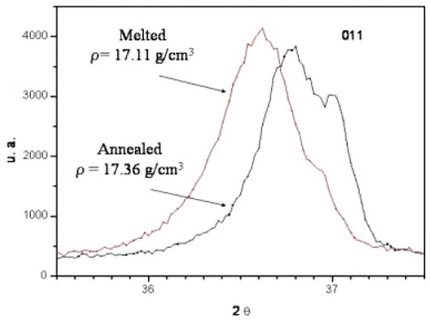

Figure 2. Evidence of stresses in γ-U7Mo shown by the displacement of the (011) DRX peak of a just melted and an annealed sample.

2.2. Low temperature hydriding of γ-UMo alloy

γ-U7Mo alloys were hydrided in a 1.5 l chamber vacuum and temperature assisted. A flow meter was used to measure the incoming hydrogen needed to keep a constant hydrogen pressure during absorption. In the stressed sample, hydrogen can be allocated in interstitial positions in the crystal structure (solubilization) or in hydrogen traps in dislocations generated by tension stresses. Traps must be filled with hydrogen to allow massive hydriding of γ-UMo afterwards. At 230°C, in a 10^{-3} torr vacuum, high purity hydrogen is introduced up to a pressure of 1 atmosphere, filling traps of the stressed γ-U7Mo alloy with some hundreds ppm of hydrogen in less than one hour [44]. Lowering the temperature to 120°C, hydrogen absorption begins after a few minutes; typical hydrogen absorption rates can reach values higher than 1 liter of hydrogen gas—at standard temperature and pressure—per minute per kilogram of alloy. After several hours, hydriding is completed. Hydrogen absorption dependence with time is shown in **Figure 3**. Additional temperature controls are needed during the process since the hydriding reaction is exothermic.

http://dx.doi.org/10.5772/63652

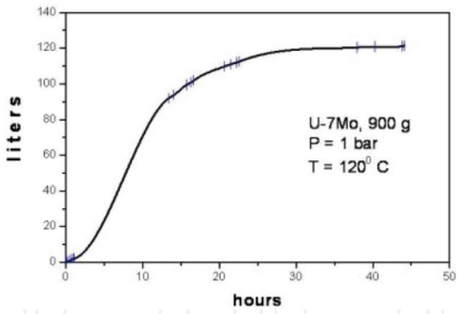

Figure 3. γ-U7Mo time dependence absorption of gaseous hydrogen at 120°C.

Optimum hydriding conditions were set up by observing the different hydrogen pick up rates in an increasing temperature slope and in a decreasing one, after hydrogen saturation of traps at 230°C. In **Figure 4**, it can be observed that hydrogen absorption rate while heating has a maximum value of 220 ppm/l and while cooling is much higher, 650 ppm/l, for a 700 g batch. From this curves it was determined that hydriding conditions were between 50 and 190°C, and the maximum rate is at 120°C.

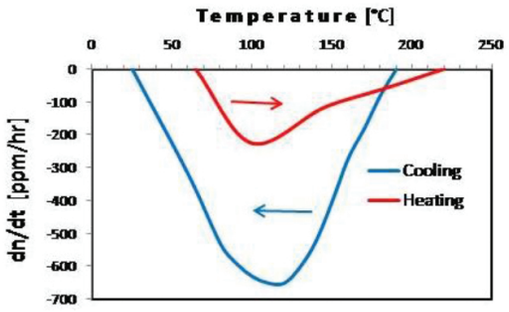

Figure 4. Hydrogen absorption rates during heating and cooling of a γ-U7Mo batch.

If a piece of γ-UMo is heated above 230°C in a hydrogen atmosphere, tension stresses will appear as it is cooled, inducing the massive hydriding of the material. This explains why in a cooling cycle hydrogen absorption is higher than in a heating one [42]. U10Mo has also been hydrided with similar results utilizing selected heating and cooling cycles such that hydriding conditions can be reached without initially incorporating residual stresses [45, 46].

After the hydride is totally formed at 120°C, it is convenient to increase the temperature up to 325°C and evacuate the chamber to eliminate the hydrogen in traps; this procedure makes the hydride less pyrophoric. Finally, at room temperature, air is introduced in a temperature controlled way such that the hydride is passivated.

2.3. Characterization of the γ-UMo hydride

The γ-U7Mo hydride is dark gray, brittle, fragmented in platelets, with small transgranular cracks (**Figure 5**). It is pyrophoric and burns with flame because of hydrogen liberation. When oxidized in air, it is dark brown. Rietveld refinement of a X-Ray diffraction—XRD—pattern

(**Figure 6**) show wide peaks corresponding to a unique stressed crystalline cubic *A-15* structure (space group $Pm\bar{3}n$, *N° 223*) of the β-W prototype, the same as β-UH_3 [47, 48] with eight heavy atoms in its unit cubic cell with parameter 6.6598 Å; the stoichiometry is of (U7Mo)H_{3-y} with values of *y* smaller than 0.2 obtained experimentally by weight difference. The XRD hydride density is 10.39 g/cm^3. Since the density of γ-U7Mo with a unit bcc cell parameter of 3.4785 Å is 17.5 g/cm^3, the increase in volume during hydriding is 68%, causing the fragmentation of the brittle hydride that is being formed.

Figure 5. γ-U7Mo hydrided fragments.

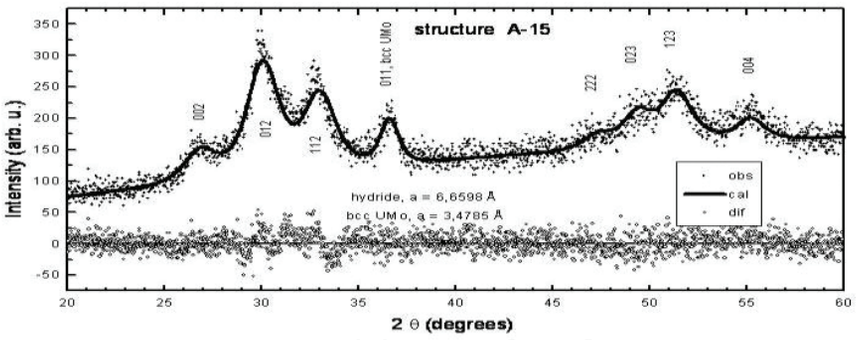

Figure 6. XRD, Rietveld refinement and indexation of (U7Mo)H_3 A-15 structure.

2.4. Milling of the γ-UMo hydride

Vickers hardness of the hydride (U7Mo)H_3 is approximately 300 VH. This hydride must be milled in a sufficient inert atmosphere to avoid burning up. Low impact mills are preferred to avoid excess fines (particle size smaller than 45 μm). Two roll mills and/or conical vibratory crushers were used (**Figure 7**). Hydride was first reduced with a manual roll mill in a glove box with less than 5% oxygen (mesh #10, 2 mm opening). These particles were then passed once through a conical crusher in a dynamic inert atmosphere reducing the size (#120, 125 microns). **Figure 8** shows hydride (γ-U7Mo)H_3 milled particles of 80 μm mean size. Passivation is needed before exposing the particles to air.

http://dx.doi.org/10.5772/63652

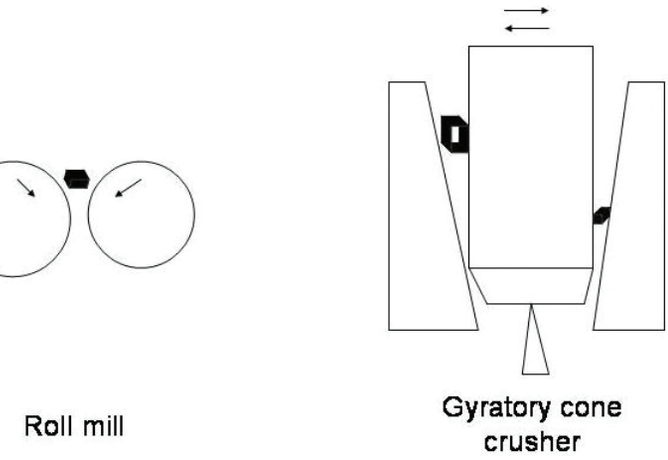

Figure 7. Low impact mills: roll (left) and gyratory cone (right).

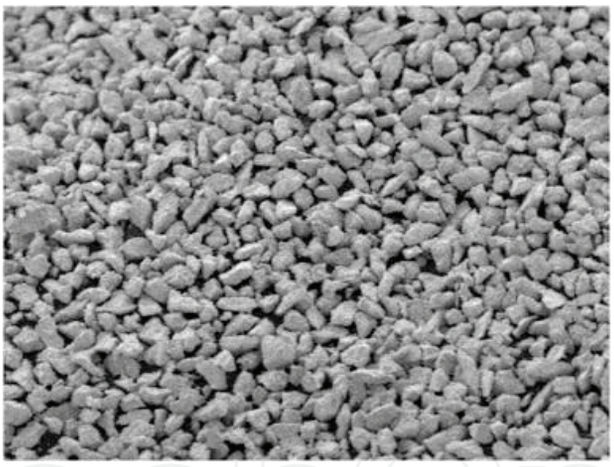

Figure 8. (U-7Mo)H_3 powder of 80 μm mean size. SEM.

2.5. (U7Mo)H_3 dehydriding

The dehydriding of the powder is done in a vacuum atmosphere with a decrease of hydride size that is important because of the density difference with the final γ-U7Mo powder. Any gas evolution is followed by pressure measurements with a closed chamber; periodic evacuation is performed to reduce excess pressure. Hydrogen liberation begins at 125°C and beyond 425°C can be bursting. The hydrogen in traps—that is incorporated at 230°C—is liberated at temperatures between 300 and 375°C, whereas the hydrogen in interstitial sites—incorporated at 120°C—will begin to be evacuated at temperatures above 380°C as shown in **Figure 9**. If,

after hydriding, hydrogen in traps is removed as mentioned in 2.2., the bump of hydrogen pressure increase at 325°C will not be observed.

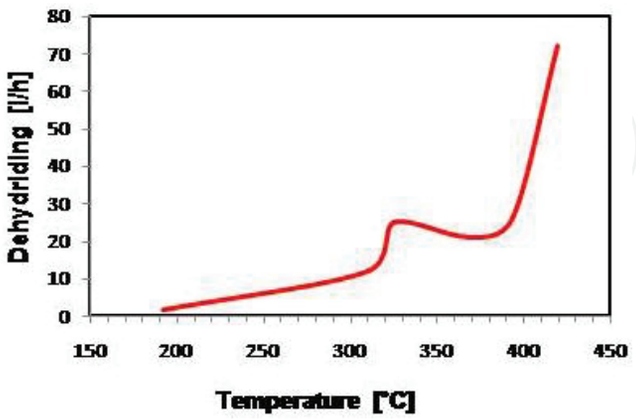

Figure 9. Hydrogen evolution during dehydriding. Hydrogen in traps and interstices are liberated around 325°C and beyond 425°C, respectively.

To eliminate hydrogen to lower values than 50 ppm heating up to 700°C in a dynamic vacuum atmosphere during 2 hours is needed. The heating chamber was vibrated to avoid the sintering of the particles. When the dehydriding is finished, an inert gas is introduced and quick cooling to room temperature is needed to quench the metastable γ-U7Mo phase. Controlled passivation is done by slow removal of the inert gas and air introduction. Dehydriding needs at least 5 hours. Cracks formed during the hydriding process are still present after dehydriding (**Figure 10**). The powder must be kept in an inert atmosphere to avoid oxidation.

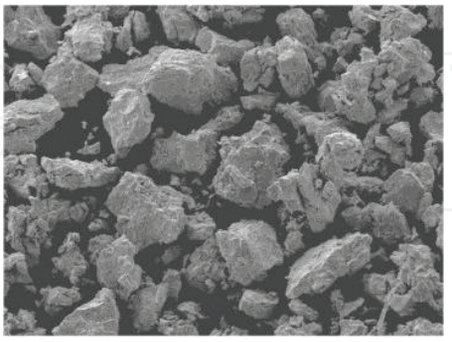

Figure 10. HMD γ-U7Mo powder. Big particles are 100 μm size (SEM).

If it is of interest, cracks can be sintered with a heat treatment of 8 hours at 1000°C in a vacuum atmosphere in the vibrating chamber [44]. **Figure 11** shows the results of this treatment.

http://dx.doi.org/10.5772/63652

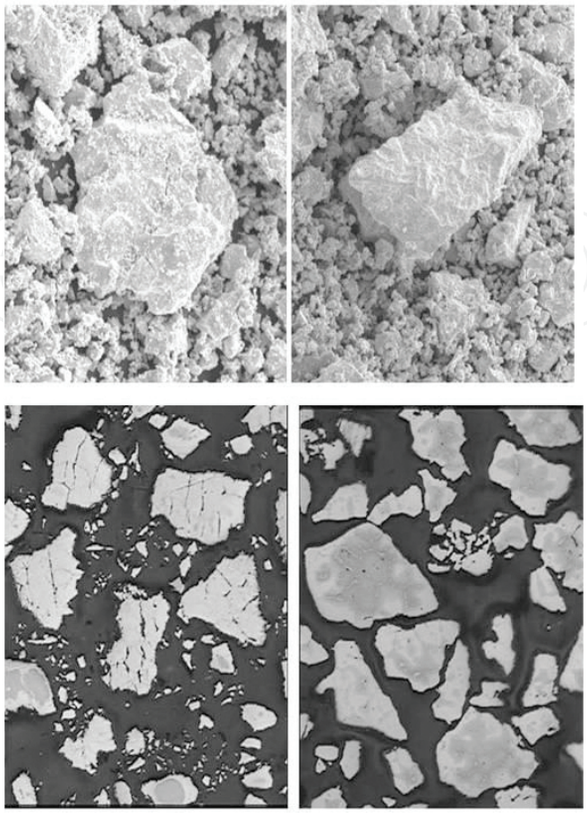

Figure 11. SEM (first row) and metallographies (second row) of γ-U7Mo powder before (left column) and after (right column) heat treatment at 1000 °C in a vacuum atmosphere. Big particles are 100 μm.

2.6. Absorption, coverage and lamination

The surface absorption of HMD powder in an air atmosphere was studied by increasing the temperature in a closed vibrating chamber. The volume of the chamber and piping was of approximately 3 liters and runs with 64 and 130 grams of γ-U7Mo HMD powder were performed [49]. **Figure 12** shows the pressure evolution from an initial value of 800 mbar air atmosphere as temperature is increased up to 500°C. The initial increment in pressure corresponds to surface gas desorption, fundamentally water at 120°C. A first run with 64 g showed an important pressure reduction up to a value of 200 mbar. Two consecutive runs were performed with a fresh 130 g sample of γ-U7Mo to evaluate if equilibrium is reached or a diffusion barrier was formed. The first run with this second batch, curve 130 g in **Figure 12**, was heated up to equilibrium. The second run, curve 130 g bis, was performed after cooling and reintroducing air in the chamber. These last two runs showed that pressure equilibrium was achieved without reaching saturation. Oxygen and nitrogen were incorporated without presenting a barrier to gas diffusion; nitrogen incorporation is known that begins to be important at temperatures higher than 300°C in metallic uranium [40]. A similar scenario will be present inside a picture and frame ensemble before hot rolling.

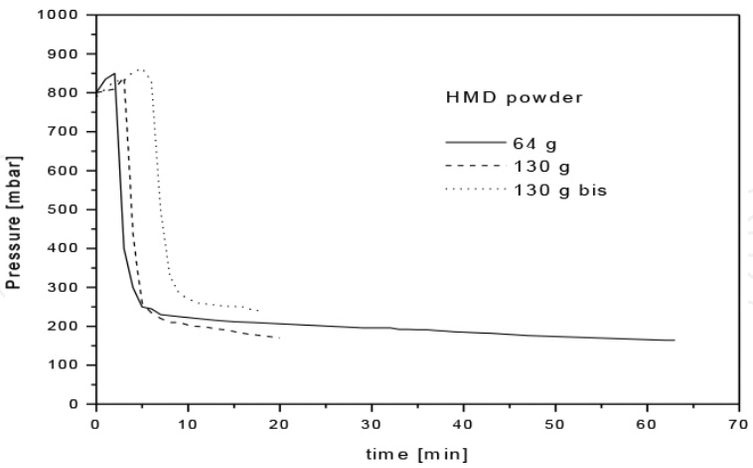

Figure 12. Pressure evolution with temperature of γ-U7Mo HMD powder exposed to an air atmosphere in a closed chamber.

Coverage of γ-UMo powder is of interest not only to diminish oxidation during storage but fundamentally to have a diffusion or metallurgical barrier protection against undesirable growth of, for example, the UMo/Al interaction zone during high flux irradiation. Surrogate powders were used to initially set up equipment and coverage conditions; silicon, aluminum, magnesium and silicon were used with chemical vapor deposition and dip coating techniques [50, 51]. Physical vapor deposition [52] is another possibility of coverage technique. Mixed powders of UMo and silicon in the vibrating chamber at 950°C in vacuum during 2 hours cover the bigger UMo particles with silicon [51].

The coverage of ductile UMo particles with brittle materials is thermomechanically incompatible in layers thicker than 1 micron. Probably ductile nickel and niobium seem to be better candidates as they have been tested previously in other nuclear fuel developments. New technologies are now available that consist in particles spheroidization and coverage using an induction couple plasma equipment that nowadays can be purchased in a commercial form [53].

The brittle transgranular fractures produced during comminution of the hydride gives as result polyhedral shaped particles. **Figure 13** shows a metallography of the laminated meat of a dispersed HMD miniplate with γ-U7Mo powder in an aluminum matrix. The irregular shape of HMD particles favors the mixing with Al powder, diminishes flow segregation—compared with spherical particles—and green compacts practically have no shredding. Cracks in the HMD particles do not propagate during hot lamination since UMo is a ductile alloy. Final porosity of a meat with HMD powder is between 5 and 10% v/v. Dispersed UMo particles in an aluminum matrix miniplates were also colaminated using silicon covered U7Mo HMD powder and centrifugal atomized particles with LEU and natural uranium [51].

http://dx.doi.org/10.5772/63652

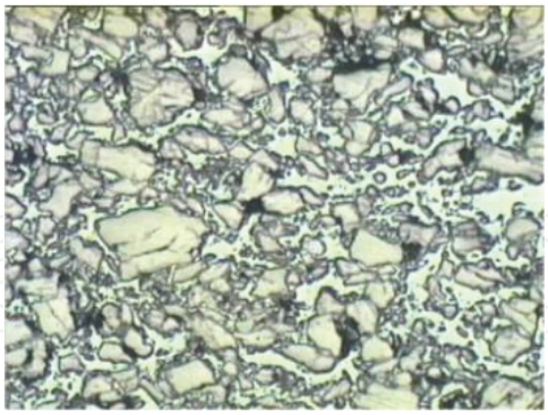

Figure 13. Metallography of the meat of γ-U7Mo HMD powder dispersed in an aluminum matrix of a laminated miniplate. The size of the big particle is approximately 100 microns. Holes between particles were fundamentally produced during polishing.

Monolithic UMo meats can be obtained by powder metallurgy. A coupon of U7Mo HMD powder was cold pressed and surrounded by AISI 304L stainless steel in the standard lids and frame configuration to conform the cladding (**Figure 14**). Colamination was performed at 675°C, a temperature in the gamma phase stable zone of the U7Mo, in a nitrogen atmosphere. The use of a UMo monolithic meat elaborated by powder metallurgy allows an easier way of obtaining different meat widths in the same plate using conformational dies, incorporation of powdered neutron moderators such as high temperature stable hydrides, burnable poisons and also nanosized porous powders to adsorb fission gases at grain boundaries so as to reduce overall swelling of fuel plates [54].

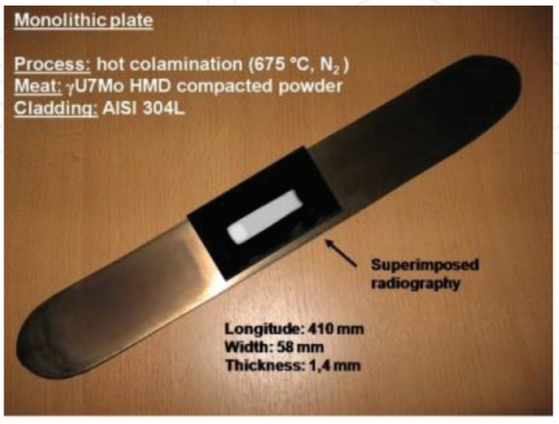

Figure 14. Monolythic UMo miniplate with stainless steel cladding.

3. Monolithic γ-UMo miniplates with cladding of Zircaloy-4

UMo and aluminum have interlayer incompatibility under irradiation and different thermo-mechanical properties that complicates a monolithic plate fabrication. These conditions can be avoided if the aluminum is replaced by a more friendly material with UMo such as Zircaloy-4, used in fuel tubes in power nuclear reactors [49, 50]. UMo has low plastic deformation compared with Zry-4; the latter has a coefficient of thermal expansion (6.10^{-6} °C^{-1}) less than half of the UMo coefficient [55]. Probably for this reason never before hot rolling colamination was applied to the system UMo/Zry, although UMo alloys have been co-extruded with Zircaloy-2 in plate and rod shapes [40, 56]. Hot rolling colamination needs several deformation steps while coextrusion is performed at higher temperatures in only one deformation step. The interaction zone growth kinetics between UMo and Zry is well known [40] and more recently it was shown by calculation that there exists a low interaction between Zr and UMo alloys [57]. Finally, a fabrication technique was developed [51], and two fuel miniplates were produced, irradiated and the post irradiation examination (PIE) was performed [43, 54, 58, 59].

3.1. Colamination parameters

Colamination temperature was chosen around 650°C where γ-UxMo phase is stable and Zry-4 is in α phase (<850°C) minimizing oxide layer growth in an air atmosphere. A uranium 7% (w/w) molybdenum alloy was chosen to maximize uranium content. Total welding in the sandwich hot colamination can only be achieved through sequential deformation steps. Differential contraction of UMo and Zry-4 in the cooling between colamination steps was avoided by quick reentrance to the heating furnace. It is illustrative to repeat a detailed description of this process mentioned in reference [43]: "The process of furnace extraction, lamination and placement again in the furnace was carried out as quickly as possible minimizing contact with cold surfaces. Thickness measurements were replaced by a very fast measurement of the plate length with a ruler from which the reduction pass was calculated. If the reintroduction in the furnace is not quick enough, repeated "crick" sounds are heard, indicating the breaking of the partial welds that were formed. After several steps, the contact surfaces are totally welded. The involved difference in contraction after final cooling are of the order of 1% and the stresses involved are absorbed by plastic deformation, as it is clear from past successful extrusion experiences. Very different sounds are heard when dropping good and bad laminated miniplates in a table: an'applause' sound stands for not totally welded surfaces, while a metallic sound is heard with a 100% surface welded miniplates. Welding between meat and frame was checked by destructive metallographic techniques."

3.2. Fabrication of miniplates

After several testing developments steps of the hot co-lamination processes (**Figure 15**), two monolithic LEU γ-U7Mo fuel miniplates with Zry-4 cladding were fabricated in CNEA for irradiation in the Advanced Testing Reactor (ATR) at Idaho National Laboratory (INL). Miniplates final size was 100 x 25 mm with a total thickness of 1 mm; nominal meat thicknesses were 0.25 (MZ25) and 0.50 (MZ50) with 0.36 and 0.25 mm of cladding thickness, respectively.

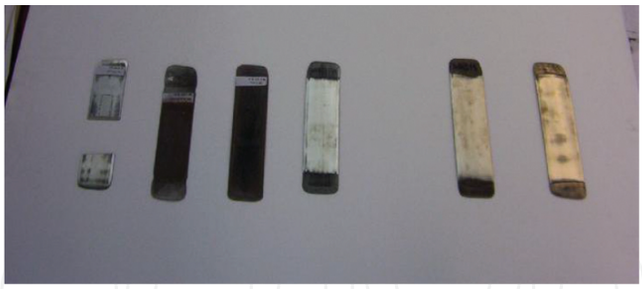

Figure 15. Monolithic γ-U7Mo/Zry-4 miniplates used along the different development stages. The three at the right extreme are in an intermediate step of surface oxide removal.

3.2.1. Alloy melting and sandwich preparation

The LEU uranium molybdenum alloy for the MZ25 and MZ50 miniplates was melted in the same way as described for powder production in section 2.1. using a graphite vertical mold to cast a 75 x 100 mm^2 plate of 2 mm thickness. Sandwich preparation was performed using the lids and frame technique thoroughly described in a previous work [43]; overall thickness of both packs was 4 mm (**Figures 16** and **17**)

Figure 16. Finished frames, lids and coupons of MZ25 and MZ50 ready to be stacked and welded to conform the two sandwiches.

Figure 17. TIG welded sandwich of monolithic U7Mo meat and Zry-4 clad ready for hot co-lamination.

3.2.2. Colamination of UMo with Zry-4

Both Zry-4/U7Mo/Zry-4 stacked plates TIG welded (sandwich) were hot colaminated using 150 mm rolls. The Stanat rolling mill had entrance guides to quickly position plates that were heated at a temperature of 675°C in an air atmosphere. To minimize the oxide layer growth the heating time between passes was set up at minimum values that could guarantee tension relieving and recrystallization of UMo. Totally welded interfaces ND near final thickness were reached after eight passes. Mean reduction step was 17.5% and mean heating time was 7.5 min; all the colamination process takes a total time of one hour. The cooling after the last lamination step must guarantee the retention of the metastable γ-U7Mo phase.

3.2.3. Final procedures

After the hot colamination, the plates were straightened in a multi roller machine and the oxide layer must be removed. Wet silicon carbide sand papers were used for this last purpose. The final thickness was reduced in 0.1 mm with the oxide layer removal and surface polishing.

Ultrasonic testing was performed to control 100% welding, and X-Ray radiography was used for checking meat dimensions, density homogeneity, dog boning, meat folding, etc. Cutting to obtain final dimensions was done with a guillotine. Identification of the miniplates was the last step of the fabrication procedure (**Figure 18**).

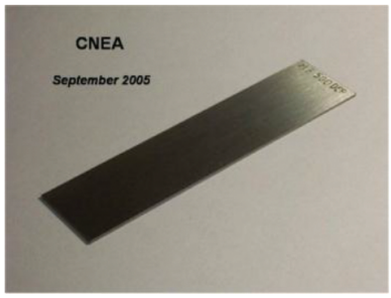

Figure 18. γ-U7Mo/Zry4 finished mini-plate of 100 x 25 x 1 mm^3 size. Meat and cladding thickness are 0.50 and 0.25 mm, respectively.

3.3. Monolithic miniplates characteristics and irradiation

The final characteristics of miniplates MZ25 and MZ50 are summarized in **Table 1** showing plate and cladding thickness, the dimensions and density of the monolithic γ-U7Mo meat and the total uranium with its meat uranium bulk and surface density.

Miniplate	Units	MZ25	MZ50
U enrichment	% ^{235}U	19.86	
U composition	% w/w U	92.91 ± 0.09	
Mo composition	% w/w Mo	7.04 ± 0.07	

Miniplate	Units	MZ25	MZ50
Plate thickness	mm	0.99	1.01
Cladding thickness	mm	0.36	0.25
Meat thickness	mm	0.26	0.51
Meat width	mm	18.8	18.6
Meat longitude	mm	73.0	71.0
Meat density	g/cm^3	17.7	17.3
Total U	g	5.9	10.9
Meat U density	gU/cm^3	16.5	16.2
Ratio U/surface	gU/cm^2	0.21	0.41

Table 1. MZ25 and MZ50 characteristics. Miniplates size is 25 x 100 mm^2.

Miniplates MZ25 and MZ50 were irradiated 90 effective full power days (EFPD) during the RERTR-7A test experiment in the ATR. Local burn-ups of ^{235}U were between 28.5 and 53.3% for MZ25 and between 25.2 and 48.3% for MZ50. Average total burn-ups were 37.5 and 33.1% for MZ25 and MZ50, respectively. The estimated beginning of life (BOL) thermal conditions, operating parameters, peak surface heat flux, power density generated at the beginning and end of irradiation, minimum and maximum clad surface temperatures, fission density, internal and external temperatures, heat flux and total swelling were previously shown [43, 59–63].

3.4. Post-irradiation examination

The post irradiation examination (PIE) was performed at the Hot Fuel Examination Facility of the Material and Fuel Complex (INL) [58, 59]. Plate swellings were 3.6% for MZ25 and slightly higher than 4% for MZ50 miniplate. Meat swellings of 15 and 12% were measured for MZ25 and MZ50, in accordance with fission densities. The swelling is low and uniform and consistent with other monolithic UMo plates with aluminium cladding irradiated in previous experiments (RERTR-6 and RERTR-7) with similar burn-ups.

An eddy current probe (HELMUT FISCHER model Delta Scope MP30) modified for hot cell was used for measuring the oxide thickness. Zero calibration was done using nonirradiated Zry-4. The average oxide layer thickness after irradiation was 2.6 and 3.2 +/− 0.5 μm for miniplates MZ25 and MZ50, respectively.

Figure 19 shows a montage of metallographic images of MZ25 miniplate cut transversally and polished. The arrow indicates the direction of the ATR core center. At the nearer end, the neutron flux is higher and burn-up reached 53.3%. The burn-up gradient across the width of the plate was 1.85. **Figure 20** shows a higher magnification optical image of the UMo/Zry-4 irradiated interface with fuel and clad remaining adherent and with no evidence of fission gas bubbles.

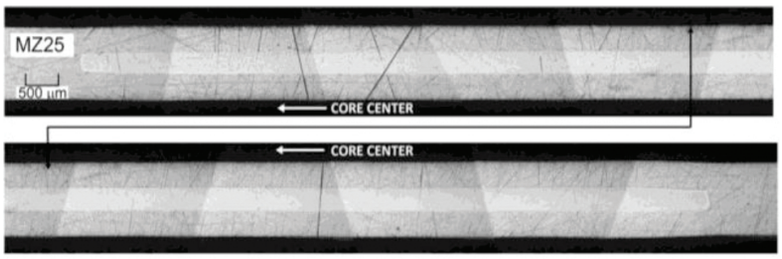

Figure 19. Optical metallographic montage of a polished transversal cut of MZ25 fuel plate.

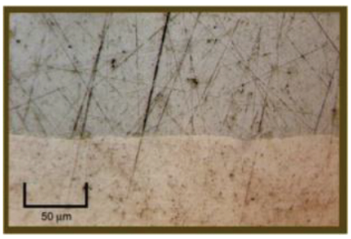

Figure 20. Metallographic cross-section of the interaction zone showing fuel (bottom) and clad (top) of MZ25 irradiated miniplate.

Figure 21 shows another high magnification optical image montage of the width end of plate MZ50 fuel/cladding interface plate that faces the ATR core centerline; a zone with the highest fission density rate and highest temperature with a 48.3% final burn-up. The width of the interaction layer between γ-U7Mo fuel and Zry-4 cladding is extremely thin and can hardly be seen. No fission gas bubbles were visible in the fuel, and the bonding between fuel and cladding is intact. The swelling is uniform.

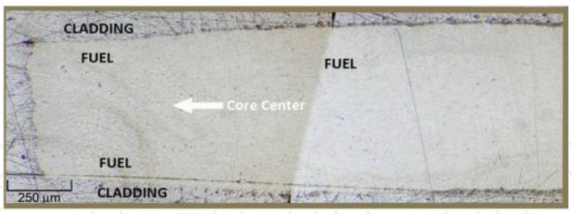

Figure 21. Metallographic cross-section of a hot zone in MZ50 miniplate.

PIE reports in both miniplates states that the fuel/clad bonding looks excellent.

4. Discussion

4.1. HMD γ-U7Mo powder performance

Hydriding in the presence of stresses can be easily corroborated using two annealed probes of γ-U7Mo, one of which has been indented after the heat treatment with a Vickers hardness

http://dx.doi.org/10.5772/63652

tip. The beginning of hydriding can be noticed only at the indented probe after slow heating of both samples up to 300°C in a hydrogen atmosphere and slow cooling. Another way of obtaining stressed samples is by melting alloy buttons in an arc furnace with a refrigerated copper crucible. Also a stressed sample of γ-UMo can probably be cathodically charged filling with hydrogen the traps preparing the alloy for massive hydriding in an hydrogen atmosphere.

Microscopic fractures are produced during the hydriding of γ-U7Mo without producing a nanosized powder as it happens with the hydriding of pure uranium. The rate of hydrogen incorporation during massive hydriding of γ-U7Mo is greater than a square root dependence with temperature because of fragmentation of the material in the phase transformation. Hydrogen incorporation increases with pressure with no variation in the absorption temperature range. UMo samples with higher purity take less time for total hydride formation [64].

The vibrating chamber allowed many of the thermal treatments at temperatures above 500°C avoiding powder sintering. The vibration was connected during hydriding, dehydriding and passivation for moving the interior material, enhancing diffusion and increasing cooling rates for quenching the metastable gamma phase. Vibration was also used for testing different coverage techniques with surrogate and UMo particles.

The oxidation kinetics of γ-UMo alloy is lower than in pure uranium. The hydride can spontaneously burn at room temperature in air. The burning of the hydride is reduced after heating in vacuum at 325°C with the elimination of hydrogen in traps. In all experiments the temperature control was performed with a thermocouple immersed in the powder, allowing immediate control of hydriding (exothermic), dehydriding (endothermic) and passivation (exothermic) processes. Direct pressure control was achieved by maintaining the chamber closed, when possible; evolution of pressure can be directly correlated with hydrogen absorption and desorption. Powders of γ-U7Mo in contact with air diminish their density from one year to another evidencing surface oxidation and hitherto should be kept in inert atmosphere containers.

4.2. Performance of monolythic γ-UMo fuel with nonaluminum cladding

Special precautions must be taken to allocate UMo monolithic coupons in the frame with very small tolerances to avoid blistering formation during the lamination process. As usual, surface contaminations of any kind—in the assembling of the fuel coupon with the lids and frame, in the welding of the sandwich, in the cleaning of the casting molds, in the maintenance of fresh reactives, etc.—must be avoided. Colamination of monolythic UMo with Zry-4 or stainless steel used as cladding materials is performed at temperatures higher than 650°C where the gamma UMo high temperature phase is stable. No special precautions are needed to avoid decomposition at working temperatures and TTT diagrams are used only in the evaluation of final cooling velocities to retain the γ-UMo phase.

The different coefficients of thermal expansion of U7Mo and Zry-4 needed a special procedure of not allowing the cooling at intermediate steps of hot Colamination. When finally cooling to room temperature with 100% welded interfaces, the appearing stresses produced by differential contraction coefficients will be absorbed by elastic or plastic deformation of Zry-4; they

probably disappear during final straightening and polishing or even during irradiation. No special treatment is needed and this is not an issue. In the case of stainless steel claddings, there is no great mismatch between thermal coefficients, and no problems are presented during hot colamination with monolithic UMo.

Nonaluminum monolithic fuel plates need to be straightened after hot lamination. More power machinery than with aluminum dispersed fuel plates is needed. The oxide layer of the Zry-4 cladding after hot colamination could only be removed by mechanical means. Since sand blasting must be done in an inert atmosphere, wet sand papers were used semimanually. In the case of stainless steel claddings the polishing can be assisted with chemical means. A more industrialized polishing can be performed using a scanning abrasive water blasting that can follow small surface deformations maintaining uniform cladding thickness. Also abrasive powders assisted by brushes can be used.

Nonaluminum claddings in UMo monolithic fuels can be smaller than 150 μm [9]. MZ50 miniplate had a cladding thickness of 250 μm and a total plate thickness of 1 mm. This cladding reduction thickness can compensate lower thermal conductivity, compared with aluminum alloys, in heat extraction. The reduction of cladding and fundamentally plate thickness can help in new designs introducing a more satisfactory adjustment of neutron moderation ratios.

The growth kinetics of oxide layer in Zry-4 and stainless steel claddings during irradiation is much lower than in aluminum claddings. The lids and frame process of monolithic γ-UMo with nonaluminum cladding using the lids and frame hot colamination fabrication process can be scaled up to full size plates.

5. Conclusions

The development of the HMD process was carried out with the production of more than 5 kg of γ-UMo powder. Basic research is still needed to study thermodynamic properties of the just discovered hydride. Equilibrium stoichiometry, hydrogen allocation in traps and interstitial positions need more elaborated studies. Scalability of the HMD UMo powder production using enriched uranium is possible up to mass batches compatible with security standards, requiring low man-power and equipment investment.

Many coverage techniques can be applied to UMo particles with different objectives and results. There is a great versatility of methods that have not all been tested under irradiation, but it seems that more focused research is needed.

The traditional picture and frame technique for the fabrication of monolithic γ-UMo plates can be used if aluminum cladding is replaced by Zircaloy-4 or AISI 304L. This is a flexible and practical production scale technology that can be used for fuels with densities greater than 17 gU/cm^3. Monolithic γ-U7Mo with Zry-4 cladding miniplates irradiated up to 50% burn up show, in PIE results, a gentle interaction zone without bubble nucleation. The monolithic UMo coupon can be fabricated from powder, with the possibility of blending burnable poisons, inert powders, gas adsorption materials, and conforming special geometrical shapes.

Conversion of high flux reactors from HEU to LEU can be done using UMo monolithic fuel technology. Usual equipment can be used with small modifications for fuel fabrication at industrial scale. Other benefits can probably be achieved by thorough evaluation of the fuel cycle up to the analysis of back end options that can bring some other benefits. Reduction in cladding and plate thickness can open the door for new designs and HEU-LEU conversion possibilities.

Author details

Enrique E. Pasqualini*

Address all correspondence to: pascua@cnea.gov.ar

Sabato Institute (UNSAM/CNEA). Nuclear Nanotechnology Laboratory, Constituyentes Atomic Center, Argentina

References

[1] Nuclear Power Reactors in the World. Reference Data Series No 2. 2015 Edition. IAEA. http://www-pub.iaea.org/MTCD/Publications/PDF/rds2-35web-85937611.pdf and https://www.iaea.org/pris/

[2] Handbook of Nuclear Engineering. Editor Dan Gabriel Cacuci. Springer Science +BusinessMedia LLC (2010). http://www.springer.com/us/book/9780387981307

[3] Research Reactor Data Base. IAEA (2009). https://nucleus.iaea.org/RRDB/RR/ReactorSearch.aspx

[4] Personal communication with F. M. Marshall of the Research Reactor Section, International Atomic Energy Agency.

[5] L. Kowarski. Report on Research Reactors. Proceedings of the International Conference on the Peaceful Uses of Atomic Energy. Vol. II, 233–247. Geneva (1955).

[6] J. R. Huffman. The Materials Testing Reactor. Nucleonics, 12, 20–26 (1954).

[7] J. E. Cunningham and E. J. Boyle. MTR-Type Fuel Elements. Proceedings of the International Conference on the Peaceful Uses of Atomic Energy. Vol. IX, 203–207. Geneva (1955).

[8] C. E. Weber and H. H. Hirsch. Dispersion Type Fuel Elements. Proceedings of the International Conference on the Peaceful Uses of Atomic Energy. Vol. IX, 196–202. Geneva (1955).

[9] J. Howe. The Metallurgy of Reactor Fuels. Proceedings of the International Conference on the Peaceful Uses of Atomic Energy. Vol. IX, 179–195. Geneva (1955).

[10] O. J. Wick, T. C. Nelson and M. D. Freshley. Plutonium Fuels Development. Proceedings of the International Conference on the Peaceful Uses of Atomic Energy. Vol. VI, 700–709. Geneva (1955).

[11] A. M. Weinberg, T. E. Cole and M. M. Mann. The MTR and Related Research Reactors. Proceedings of the International Conference on the Peaceful Uses of Atomic Energy. Vol. II, 402–419. Geneva (1955).

[12] C. B. Waff. Administration pushes alternative nuclear fuel cycles. Phys. Today 32, 2, 85 (1979). http://scitation.aip.org/content/aip/magazine/physicstoday/article/32/2/10.1063/1.2995433

[13] RERTR, Reduced Enrichment for Research and Test Reactors. US DOE.http://www.rertr.anl.gov/

[14] J. P. Schwartz. Uranium Dioxide Caramel Fuel. An Alternative Fuel Cycle for Research and Test Reactors. International Conference on Nuclear Non-Proliferation and Safeguards. New York (1978). https://www.oecd-nea.org/science/docs/1978/neacrp-l-1978-214.pdf

[15] Research Reactor Core Conversion. From the Use of Highly Enriched Uranium to the Use of Low Enriched Uranium Fuels. Guidebook. Technical Document, IAEA (1980). http://www-pub.iaea.org/MTCD/publications/PDF/te_233_web.pdf

[16] T. D. Ippolito Jr. Effects of Variation of Uranium Enrichment on Nuclear Submarine Reactor Design. MIT, USA (1990). http://fissilematerials.org/library/ipp90.pdf

[17] A. G. Samoilov, A. I. Kashtanov and V. S. Volkov. Dispersion-Fuel Nuclear Reactor Elements. Atomizdat, Moskva 1965. Translated from Russian, Jerusalem (1968).

[18] G. L. Hofman, J. Rest, and J. T. Snelgrove. Comparison of Irradiation Behavior of Different Uranium Silicide Dispersion Fuel Element Designs. International Meeting on Reduced Enrichment for Research and Test Reactors. Williamsburg, Virginia, USA (1994). http://www.osti.gov/scitech/servlets/purl/10107567/

[19] NUREG 1313. Safety Evaluation Report Related to the Evaluation of Low-Enriched Uranium Silicide-Aluminum Dispersion Fuel for Use in Non-Power Reactors. U.S. Nuclear Regulatory Commission Office of Nuclear Reactor Regulation (1988). https://www.iaea.org/OurWork/ST/NE/NEFW/Technical-Areas/RRS/documents/mo99/NUREGfuelexp1988.pdf

[20] K. H. Kim, D. B. Lee, Ch. K. Kim, I. H. Kuk and K. W. Paik. Characteristics of U3Si and U3Si2 Powders Prepared by Centrifugal Atomization. J. Nucl. Sci. Technol. 34, 12, 1127–1132 (1997).

[21] J. L. Snelgrove, G. L. Hofman, C. L. Trybus, and T. C. Wiencek. Development of Very-High Density Fuel by the RERTR Program. International Meeting on Reduced Enrich-

ment for Research and Test Reactors. Republic of Korea (1996). http://www.rertr.anl.gov/FUELS96/SNELGR96.PDF

[22] Good Practices for Qualification of High Density Low Enriched Uranium Research Reactor Fuels. IAEA Nuclear Energy Series N° NF-T-5.2 (2009). http://www-pub.iaea.org/MTCD/publications/PDF/pub1400_web.pdf

[23] G. L. Hofman and M. K. Meyer. Design of High Density Gamma-Phase Uranium Alloys for LEU Dispersion Fuel Applications. International Meeting on Reduced Enrichment for Research and Test Reactors. Brazil (1998). http://www.rertr.anl.gov/Fuels98/GHofman.pdf

[24] M. K. Meyer, G. L. Hofman, J. L. Snelgrove, C. R. Clark, S. L. Hayes, R. V. Strain, J. M. Park and K. H. Kim. Irradiation Behavior of Uranium-Molybdenum Dispersion Fuel: Fuel Performance Data from RERTR-1 and RERTR–2. International Meeting on Reduced Enrichment for Research and Test Reactors. Budapest, Hungary (1999). http://www.rertr.anl.gov/Web1999/PDF/09Meyer99.pdf

[25] S. Van den Bergue, W. Van Renterghem and A. Leenaers. Transmission Electron Microscopy Investigation of Irradiated U-7 wt% Mo Dispersion Fuel. International Meeting on Reduced Enrichment for Research and Test Reactors. Prague, Czech Republic (2007). http://www.rertr.anl.gov/RERTR29/PDF/13-2_VandenBerghe.pdf

[26] G. L. Hofman, M. K. Meyer and A. E. Ray. Design of High Density Gamma-Phase Uranium Alloys for LEU Dispersion Fuel Applications. International Meeting on Reduced Enrichment for Research and Test Reactors. Sao Paulo, Brazil (1998). http://www.rertr.anl.gov/Fuels98/GHofman.pdf

[27] R. J. Van Thyne and D. J. McPherson. Transformation Kinetics of Uranium-Molybdenum Alloys. Transactions of the American Society for Metals, 49, 598–619 (1957).

[28] J. M. Hamy, F. Huet, B. Guigon, P. Lemoine, C. Jarousse, M. Boyard and J. L. Emin. Status as of October 2003 of the French UMo Group Development Program. International Meeting on Reduced Enrichment for Research and Test Reactors. Chicago, Illinois, USA (2003). http://www.rertr.anl.gov/RERTR25/PDF/Lemoine.pdf

[29] G.L. Hofman, Y.S. Kim, M.R. Finlay and J.L. Snelgrove. Recent Observations at the Postirradiation Examination of Low-Enriched U-Mo Miniplates Irradiated to High Burnup. International Meeting on Reduced Enrichment for Research and Test Reactors. Chicago, Illinois, USA (2003). http://www.rertr.anl.gov/RERTR25/PDF/Hofman.pdf

[30] P. Lemoine, J. L. Snelgrove, N. Arkhangelsky and L. Alvarez. UMo Dispersion Fuel Results and Status of Qualification Programs. International Topical Meeting on Research Reactor Fuel Management (RRFM). München, Germany (2004). http://www.iaea.org/inis/collection/NCLCollectionStore/_Public/35/036/35036191.pdf

[31] G. L. Hofman, M. R. Finlay and Y. S. Kim. Post-Irradiation Analysis of Low Enriched U-Mo/A1 Dispersions Fuel Miniplate Tests, RERTR 4 & 5. International Meeting on

Reduced Enrichment for Research and Test Reactors. Vienne, Austria (2004). http://www.rertr.anl.gov/RERTR26/pdf/10-Hofman.pdf

[32] T. C. Wiencek and I. G. Prokofiev. Low-Enriched Uranium-Molybdenum Fuel Plate Development. International Meeting on Reduced Enrichment for Research and Test Reactors. Las Vegas, Nevada, USA (2000). http://www.rertr.anl.gov/Web2000/PDF/Wien00.pdf

[33] C. R. Clark, S. L. Hayes, M. K. Meyer, G. L. Hofman and J. L. Snelgrove. Update on U-Mo Monolithic and Dispersion Fuel Development. International Topical Meeting Research Reactor Fuel Management. München, Germany. 41–45 (2004). http://www.euronuclear.org/pdf/RRFM%202004%20Session%202.pdf

[34] G. A. Moore, B. H. Rabin, J. F. Jue, C. R. Clark, N. E. Woolstenhulme, B. H Park, S. E. Steffler, M. D. Chapple, M. C. Marshall, J. J. Green, and B. L. Mackowiak. Development Status of U10Mo Monolithic Fuel Foil Fabrication at the Idaho National Laboratory. International Meeting on Reduced Enrichment for Research and Test Reactors. Lisbon, Portugal (2010). http://www.rertr.anl.gov/RERTR32/pdf/S12-P1_Moore.pdf

[35] S. Van Den Berghe, A. Leenaers, E. Koonen and L. Sannen. From high to low enriched uranium fuel in research reactors. Adv. Sci. Technol. 73, 78–90 (2010). http://www3.sckcen.be/microstructure/Research/VA-ASCT-10.pdf

[36] C. R. Clark, B. R. Muntifering, and J. F. Jue. Production and Characterization of Atomized U-Mo Powder by the Rotating Electrode Process. International Meeting on Reduced Enrichment for Research and Test Reactors. Prague, Czech Republic (2007). http://www.rertr.anl.gov/RERTR29/PDF/15-2_Clark.pdf

[37] C. R. Clark, M. K. Meyer and J. T. Strauss. Fuel Powder Production from Ductile Uranium Alloys. International Meeting on Reduced Enrichment for Research and Test Reactors. Sao Paulo, Brazil (1998). http://www.iaea.org/inis/collection/NCLCollectionStore/_Public/35/040/35040232.pdf

[38] S. Balart, P. Bruzzoni, M. Granovsky, L. Gribaudo, J. Hermida, J. Ovejero, G. Rubiolo and E. Vicente. U-Mo alloy powder obtained by a hydride-dehydride process. International Meeting on Reduced Enrichment for Research and Test Reactors. Las Vegas, Nevada, USA (2000). http://www.rertr.anl.gov/Web2000/PDF/Balar00.pdf

[39] M. I. Solonin, A. V. Vatulin, Y. A. Stetsky, Y. I. Trifonov and B. D. Rogozkin. Development of the Method of High Density Fuel Comminution by Hydride-Dehydride Processing. International Meeting on Reduced Enrichment for Research and Test Reactors. Las Vegas, Nevada (2000). USA. http://www.rertr.anl.gov/Web2000/PDF/Vatu00.pdf

[40] W. D. Wilkinson. Uranium Metallurgy. Interscience Publishers. John Wiley and Sons Inc. New York (1962).

[41] G. L. Powell. Solubility of hydrogen and deuterium in a uranium-molybdenum alloy. J. Phys. Chem., 80 (4), 375–381 (1976).

[42] E. E. Pasqualini, J. Helzel Garcia, M. López, E. Cabanillas and P. Adelfang. Powder Production of U-Mo Alloy, HMD Process. (Hydriding-Milling-Dehydriding). International Topical Meeting on Research Reactor Fuel Management. Ghent, Belgium. 183–187 (2002). http://www.euronuclear.org/meetings/rrfm/pdf/RRFM%202002.pdf

[43] E. E. Pasqualini. Alternative processes of comminution and colamination of uranium molybdenum alloys. Prog. Nucl. Energy. 75, 92–104 (2014).

[44] E. E. Pasqualini, M. López and A. Gonzalez. Set Up of U-Mo Powder Production by HMD Process. International Meeting on Reduced Enrichment for Research and Test Reactors. Vienne, Austria (2004). http://www.rertr.anl.gov/RERTR26/pdf/P11-Pasqualini.pdf

[45] M. Chen, X. Yi-fu, W. Jing, J. Jia and P. Zhang. Characterization of γ-U–10 wt.% Mo alloy powders obtained by hydride-milling-dehydride process. J. Nucl. Mat. 400, 1, 69–72 (2010).

[46] R. M. Leal Neto, C. J. Rocha, E. Urano de Carvalho, H. G. Riella and M. Durazzo. Investigation of powdering ductile gamma U-10 wt% Mo alloy for dispersion fuels. J. Nucl. Mat. 445, 218–223 (2014).

[47] H. J. Goldschmidt. Interstitial alloys. Butterworths, London (1967).

[48] International Tables for Crystallography. Volume A: Space-Group Symmetry. Editor Theo Hahn, Fifth Edition (2002). ISBN-13: 978-0792365907

[49] E. E. Pasqualini. Advances and Perspectives in U-Mo Monolithic and Dispersed Fuels. International Meeting on Reduced Enrichment for Research and test Reactors. Cape Town, Republic of South Africa (2006). http://www.rertr.anl.gov/RERTR28/PDF/S6-4_Pasqualini.pdf

[50] E. E. Pasqualini and M. Lopez. Increasing the Performance of U-Mo Fuels. International Meeting on Reduced Enrichment for Research and Test Reactors.Vienna, Austria. 2004. http://www.rertr.anl.gov/RERTR26/pdf/23-Pasqualini%20II.pdf

[51] E. E. Pasqualini. Dispersed (Coated Particles) and Monolithic (Zircaloy-4 Cladding) U-Mo Miniplates. International Meeting on Reduced Enrichment for Research and Test Reactors. Boston, USA (2005). http://www.rertr.anl.gov/RERTR27/PDF/S15-3_Pasqualini.pdf

[52] S. Van Den Berghe, A. Leenaers and C. Detavernier. Selenium Fuel: Surface Engineering of U(Mo) Particles to Optimise Fuel Performance. International Topical Meeting on Research Reactor Fuel Management. Marrakech, Morocco. 26–34 (2010). http://www.euronuclear.org/meetings/rrfm2010/transactions/RRFM2010-transactions-s2.pdf

[53] M. Boulos. New frontiers in thermal plasmas from space to nanomaterials. Nucl. Eng. Technol. 44, 1, 1–8 (2012). http://www.kns.org/jknsfile/v44/JK0440001.pdf

[54] E. E. Pasqualini. Monolithic γ-UMo Nuclear Fuel Plates with Non Aluminium Cladding. International Meeting on Research Reactor Fuel Management. Hamburg, Germany. 67–72 (2008). http://www.euronuclear.org/meetings/rrfm2008/transactions/rrfm2008-session2.pdf

[55] J. Rest, Y. S. Kim, G. L Hofman, M. K. Meyer and S. L. Hayes. U-Mo Fuels Handbook. ANL-09/31 (2009).

[56] H. J. Snyder. Fuel-Clad Bond Testing of Zircaloy-2 Clad, Uranium-12 w/o Molybdenum Fuel Rods. OSTI: 4348214. Report Number(s): WAPD-141. DOE Contract Number: AT-11-1-GEN-14. Feb 15 (1956).

[57] J. E. Garcés and G. Bozzolo. Atomistic Simulation of High-Density Uranium Fuels. Sci. Technol. Nucl. Instal. 2011, 16 (2011); Article ID 531970. http://www.hindawi.com/journals/stni/2011/531970/

[58] A. B. Robinson and M. R. Finlay. RERTR-7 Post Irradiation Examination (PIE) Letter Report. INL/EXT-07-13271. Sep. 2007.

[59] D. M. Perez, M. A. Lillo, G. S. Chang, G. A. Roth, N. E. Woolstenhulme and D. M. Wachs. RERTR-7 Irradiation Summary Report. INL/EXT-11-24283. Dec. 2011.

[60] D. M. Wachs, R. G. Ambrosek, G. S. Chang and M. K. Meyer. Design and Status of RERTR Irradiation Tests in the Advanced Test Reactor. International Meeting on Reduced Enrichment for Research and Test Reactors. Cape Town, Republic of South Africa (2006). http://www.rertr.anl.gov/RERTR28/PDF/S9-3_Wachs.pdf

[61] G. S. Chang and M. A. Lillo, "RERTR-7A As-Run Physics Analysis and Test Train Isocoveres Radiological Characterization Versus Cooling Time," EDF-6857, rev.2, INL, 2007.

[62] A. B. Robinson, G. L. Chang, D. D. Keiser, Jr., D. M. Wachs and D. L. Porter. Irradiation Performance of U-Mo Alloy Based Monolithic Plate-type Fuel – Design Selection. INL/EXT-09-15903, Rev 0 (to be published).

[63] A. Denis and A. Soba. Placa/Dplaca Simulation of Monolithic/Disperse UMo Plates. International Topical Meeting Research Reactor Fuel Management. Lyon, France. 96–100 (2007). http://www.euronuclear.org/meetings/rrfm2007/transactions/rrfm2007-transactions-postersession.pdf

[64] R. Van Houten. Selected engineering and fabrication aspects of nuclear metal hydrides (Li, Ti, Zr, and Y). Nucl. Eng. Design. 31, 434–448 (1974).